

## DESIGN AND TEST OF THE RHIC CMD10 ABORT KICKER\*

H. Hahn,<sup>#</sup> M. Blaskiewicz, A. Drees, W. Fischer, Jian-Lin Mi, Wuzheng Meng,  
 Ch. Montag, Chien Pai, J. Sandberg, N. Tsoupas, J. E. Tuozzolo, Wu Zhang  
 BNL, Upton, NY 11973

### Abstract

In recent RHIC operational runs, planned and unplanned pre-fire triggered beam aborts have been observed that resulted in quenches of SC main ring magnets, indicating a weakened magnet kick strength due to beam induced ferrite heating. An improvement program was initiated to reduce the longitudinal coupling impedance with changes to the ferrite material and the eddy-current strip geometry. Results of the impedance measurements and of magnet heating tests with CMD10 ferrite up to 190 °C are reported. All 10 abort kickers in the tunnel have been modified and were provided with a cooling system for the RUN 15.

### INTRODUCTION

The original RHIC design provided a beam abort system for machine protection comprising five kicker magnets with the associated pulsers and pulse forming networks in each ring [1, 2]. The 5 kickers are serially located in the beam vacuum and must deflect the bunches by  $\geq 3.55$  cm to reach the dump absorber, corresponding to a beam kick of 1.5 mrad or 0.252 Tm/kicker [3]. The beam is deflected horizontally, and in essence the magnet defines a  $7\sigma$  dynamic aperture. Each kicker is driven by a pulsed power supply during a 12  $\mu$ s long pulse to eject 111 bunches. The kick starts with 1  $\mu$ s rise time in the gap, formed by 9 missing bunches out of 120. The pulser is capable of 29 kV and at operation with 27 kV delivers 18 kA while modulating down to 11 kA. The required 1  $\mu$ s rise time without thyatron pre-fire depends on the reservoir heater setting [4, 5].

The abort system performance as designed for the disposal of  $\sim 200$  kJ was adequate until Run 13, when planned and thyatron pre-fired beam aborts resulted in quenching of SC main ring magnets [6, 7]. Retuning of the coiled-wire inductors in the pulse forming network provided temporary correction and allowed completion of the run. Various explanations were considered but the lowering of the pulser current bottom dip shown in Fig. 1 identified beam induced heating of the magnet inductance as the culprit. Planned p intensity increases in Run 15 from  $1 \times 10^{11}$  to beyond  $2.5 \times 10^{11}$  ppb [8] triggered the kicker redesign efforts.

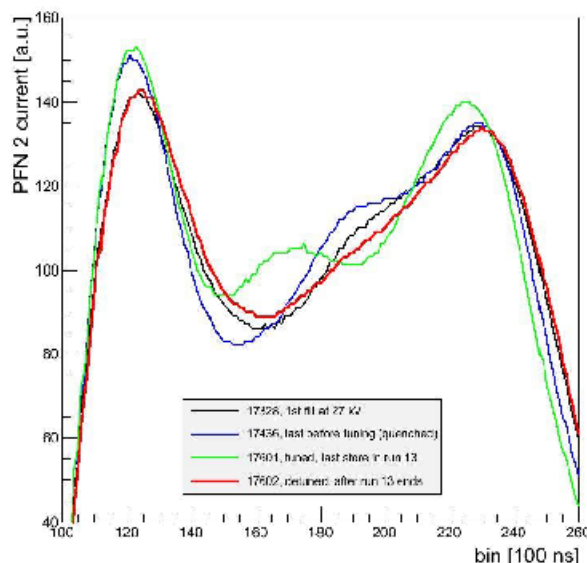


Figure 1: Pulser current at 27 kV in different operational stages: cold start, after quench, detuned in RUN13 and detuned cooled [6].

### MAGNET INDUCTANCE

The magnet current sweep range results from an impedance mismatch between pulser and abort magnet impedance,  $\omega L$ . The abort kicker inductance  $L$  has been largely determined by the dynamic beam aperture and by the power supply to be reasonably sized regarding voltage and peak current. The abort kickers are  $\ell = 1.22$  m long and are constructed as window frame magnets with an aperture of  $a = 5.08 \times b = 7.62$  cm in ferrite blocks,  $w = 2.67$  cm wide. The inductance seen by the pulser can be estimated from  $L \approx \mu_0 \frac{a\ell}{b} / (1 + a/\mu_r w)$  plus the feed-through inductance, that is the coaxial tube shown as Fig. 3 in Ref. [2]. The inductance is conveniently measured with a network analyzer via the bus bar input impedance as  $L = Z_{BB} / \omega$  and is shown in Fig. 2 for the original magnet.

The kicker heating is dominated by the  $\mu''$  component of the ferrite and the search for better material beyond CMD5005 was done at many laboratories [9, 10], although limited here to the Ni-Zn ferrite CMD10 [11].

\*Work supported by Brookhaven Science Associates, LLC under contract no. DE-AC02-98CH10886 with the DOE.  
<sup>#</sup> hahn@bnl.gov

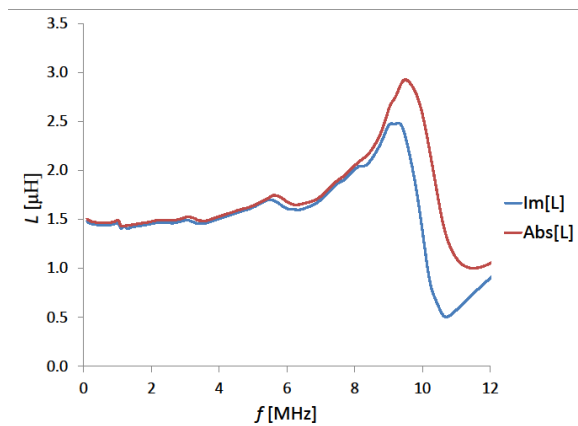


Figure 2: Inductance of the original abort kicker from the bus bar impedance taken with feed-through.

Comparing the permeability properties of the original CMD5005 and the replacement CMD10 is again possible with the bus bar measurements for the real and imaginary impedance components shown in Fig. 3. The magnet current shape results from joining the pulser output and kicker bus bar impedances. Although noticeable, the  $\mu$  differences are not dramatic and hardly justify the replacement. In contrast, the difference in Curie temperature of 130 °C and 230 °C and the associated tolerable increase in the operational temperature at maximum flux density favours using CMD10.

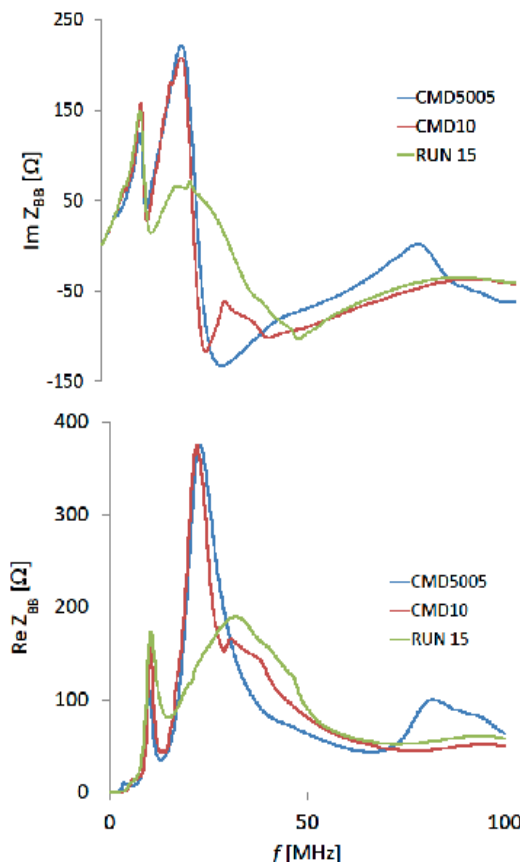


Figure 3: Bus bar impedance of abort magnets.

## MAGNET LOSS ANALYSIS

The magnet temperature increase is generated via the longitudinal kicker impedance by an axial beam. The real impedance contributions are made by various components, the imaginary  $\mu''$  component of the ferrite, the copper Eddy current strip, the stainless bus bar, and the stainless vacuum vessel. Reducing the losses requires detailed knowledge of the individual contributions that can be obtained from a two-dimensional model [12]. The numerical implementation has been done with sufficient accuracy using the “ac-module” of the 2D OPERA computer code. [13].

Fig. 4 shows the vertical cross section of the Eddy current strip plus the bus bar section of the RHIC abort kicker. The beam current is simulated as a sinusoidal function with amplitude of 1.5 A at the frequency of 10 MHz, close to the strongest RHIC beam spectrum line. The permeability of the ferrite is 220-45° and 450-45°, where 45° ~  $\mu''/\mu'$  at 10 MHz, for CMD5005 and CMD10 respectively, the latter used in RUN15.

Several geometry configurations were explored regarding losses, but had to be discarded due to high voltage arcing and study time constraints. The simulation results for the original and CMD10 magnet are tabulated in Table 1. The gain from changing the copper strip from 1 mm to 2 with a 1 mm radial end is seen by running the same kicker geometry with the same permeability.

Table 1: Simulated Magnet Losses ( $\times 10^{-4}$ W/mm)

Strip	Type	Total	Ferrite	Eddy	Bus bar
1	220-45	28.7	20.9	5.80	2.0
1	450-45	18.6	10.6	6.00	2.0
2+r1	220-45	12.71	9.22	1.49	2.0
2+r1	450-45	10.12	1.49	1.52	2.0

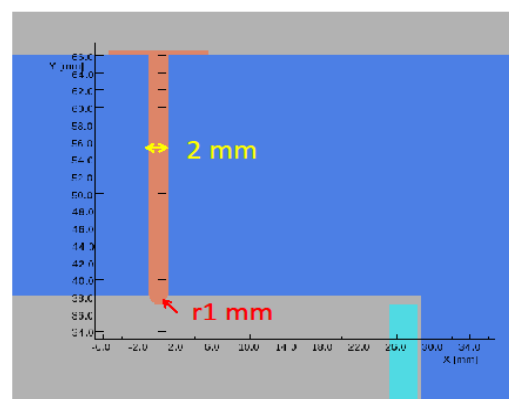


Figure 4: Eddy current strip, 2 mm wide with  $r=1$  mm half sphere end, plus bus bar for the kicker in RUN 15.

## LONGITUDINAL IMPEDANCE

Changes of the abort kicker kick strength are attributed to kicker temperature and its dependence on beam intensity. The numerical connection thereof is effectively measured by the longitudinal impedance of the abort

Content from this work may be used under the terms of the CC BY 3.0 licence (© 2015). Any distribution of this work must maintain attribution to the author(s), title of the work, publisher, and DOI.

kicker. Being of some operational interest to beam instabilities, a measurement of the longitudinal impedance had been done [14] but had to be repeated for the dimensional and ferrite changes. In the simplified test here, the impedance matching in the reference tube is substituted with ERI type-N female adaptors connecting directly to the 6.35 mm OD. rod/current tube [15]. The  $S_{21}$  signals, with the delay of 6.2 ns for the 1.86 m magnet length entered, provide the magnet impedance as the difference between data for the magnet and reference tube after conversion. The rod serves for impedance measurements and for the magnet heating tests. The direct and adjusted real and imaginary longitudinal impedance,  $Z_T$ , of the CMD10 magnet at room temperature is shown in Fig. 5.

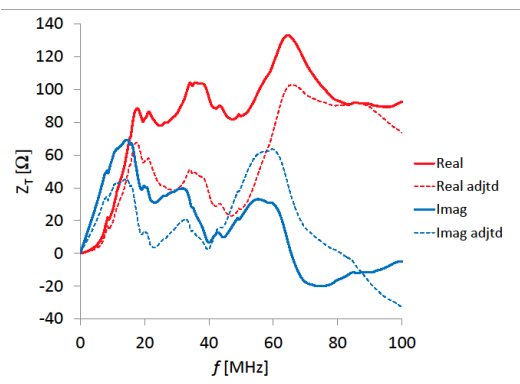


Figure 5: Kicker magnet longitudinal impedance, solid direct and dotted adjusted for reference tube.

### THE KICKER AT TEMPERATURE

Intending to establish and qualify the magnet heating as beam-generated, the magnet was excited at 30 MHz with 1 A via the rod into a 50 Ω termination. The temperature change over a 12 h period and the subsequent cooling is shown in Fig. 6. The heat capacity of the kicker is about 720 kJ of which 70 % are due to the ferrite blocks. Increasing the temperature by ~3.4 °C/h while overcoming 0.6 °C/h is done by an 80 W source, such as 1 A into the ~80 Ω of Fig. 5. To ensure cooling in operation, the ferrite blocks are enclosed with copper plates as seen in Fig. 7.



Figure 7: The kicker with Cu cooling plates in the RHIC tunnel.

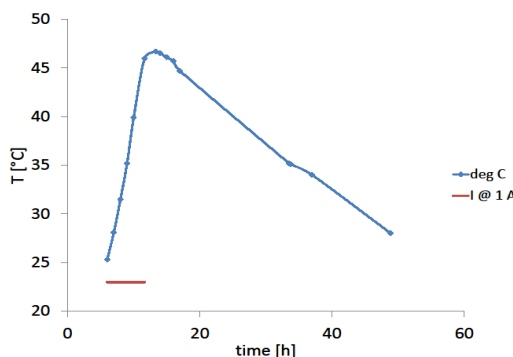


Figure 6: Magnet heating due to 1 A at 30 MHz.

### CONCLUSION

The primary goal of redesigning the abort kicker was to provide a pulse shape with adequate kick strength at the expected increased beam currents by reducing the coupling impedance and by selecting a high-Curie ferrite. To demonstrate success, the modified prototype was fully enclosed with blanking covers, heated, and pulsed beyond operational level at 27 kV up to 190 °C. Figure 8 compares the pulse current at 140 °C with that at 20 °C. The magnets have been rebuilt locally in the tunnel by changing the ferrite blocks, adding the cooling plates, and then rolling the group of five back into their vacuum tube. At a vacuum of ~10<sup>-9</sup>, the abort kicker system was transferred to the operational group.

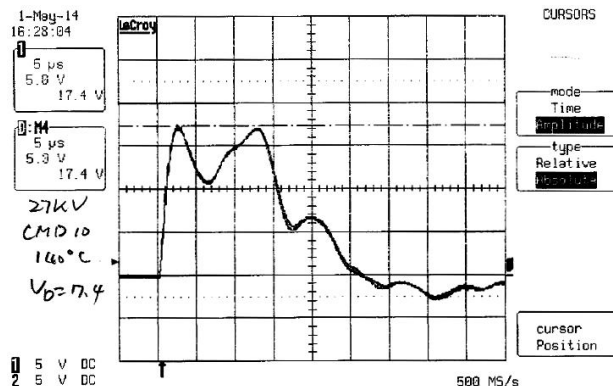


Figure 8: Current pulses in CMD10 kicker at 27 kV.

### REFERENCES

- [1] H. Hahn et al., NIM Phys. Res. A 499, p. 245 (2003).
- [2] H. Hahn et al., Proc. 1999 PAC, 2, 1999, p. 1100.
- [3] A. J. Stevens, BNL AD/RHIC/RD-94 (BNL 1995).
- [4] H. Yugang et al., BNL C-A/AP/194 (2005).
- [5] Y. Tan, S. Perlstein, Report C-A/AP/517 (2014).
- [6] A. Drees, RHIC Monday Meeting, 12/12/14.
- [7] C. Montag et al., Proc. NAPAC 2013, p. 1322.
- [8] W. Fischer et al., Proc. IPAC 2014, p. 913.
- [9] H. Hahn and D. Davino, Proc. EPAC 2002, p. 1502.
- [10] K. Fan, et al., Proc. IPAC 2012, p.3725.
- [11] Ceramic Magnetics, Inc., Fairfield, NJ.
- [12] H. Tsutsui, CERN-SL-2000-004 AP (2000).
- [13] N. Tsoupas, et al., BNL C-A/AP/524 (2014).
- [14] N.P. Abreu, et al., BNL C-A/AP/362 (2009).
- [15] Electronics Research, Inc. RLA050-NF 7/8" EIA-N.